Frequency tuning in the electroreceptive periphery

Elizabeth S. Olson and Louis D. Smullin
Department of Physics and Department of Electrical Engineering and Computer Science, Massachusetts Institute of Technology, Cambridge, Massachusetts 02139

ABSTRACT Our studies are concerned with the frequency tuning that is provided by the electrical resonance of tuberous electroreceptors. Frequency selectivity had previously been measured in the electroreceptor's afferent fibers, and resonant conductances in the electroreceptor cell membrane had been implicated in producing the selectivity. With transdermal application of sinusoidal current, we measured the frequency dependence of the impedance of small areas of the electroreceptor/skin structure of the weakly electric fish Sternopygus and Eigenmannia, and used our data to make a quantitative linear model of the structure. The qualitative form of the model was proposed by Bennett (1). The quantitative model allows us to estimate the frequency selectivity of the voltage across the innervated membrane of the electroreceptor cells. The frequency selectivity of electroreceptor cell voltage derived from our data are as sharp as the neural selectivity at frequencies close to the most sensitive frequency.

Many of our measurements supported the linear system model. However, spontaneous electroreceptor voltage oscillations were detected in some of our specimens, suggesting that the electroreceptors can operate in a regime of active nonlinearity. A simple explanation for the observed oscillations is that they arise when damping in the electroreceptor cell's resonant membrane is negative for a limited span of membrane voltage surrounding the resting voltage. The response of oscillating units to sinusoidal current was compatible with this explanation. We report experimental observations bearing on the consequences of active nonlinearity for the frequency tuning of a resonant system.

A. INTRODUCTION

Tuberous electroreceptors are voltage sensitive organs located in the skin of weakly electric fish, where they exist as a dense array that has been likened to an electrical retina. The receptors, in cooperation with current generated by a stack of electrically excitable cells located in the tail and body, make up an active electrical sensing system for use in detecting objects in the fish's nearby environment. Current generated in the electric organ, termed the electric organ discharge (EOD), passes into the water, establishing an electric field around the fish, and reenters the fish throughout the body and head. Objects in the field can be detected because they distort the distribution of current reentering the fish.

The receptors are most dense in the head where there are often $50/mm^2$. In the fish under investigation, the receptors in the trunk usually exist as clusters containing about five receptors. The density of receptors within a cluster can be even higher than the general density in the head, but there are three or fewer clusters/mm^2.

In Sternopygus and Eigenmannia, the EOD is a periodic quasisinusoidal waveform of fixed frequency, f_{EOD}. The firing response in the afferent fibers that contact tuberous electroreceptors had been shown to be selective to stimulation frequency in a band around f_{EOD}. Hopkin's data demonstrating neural frequency selectivity are in Fig. 1 (reference 2).

The tuberous electroreceptors of Eigenmannia and Sternopygus are anatomically similar. Each tuberous electroreceptor is composed of ~20 receptor cells, sitting side by side in a capsule formed by an invagination in the skin. The receptor cells are ~20 μm in length, and have a maximum width of ~8 μm. The outer membrane of a receptor cell, in contact with the lumen of the electroreceptor, accounts for ~95% of the cell area. The inner membrane is in contact with the inner milieu of the fish. The outer and inner membranes are electrically isolated from each other by means of tight junctions between receptor cells and adjacent cells (supporting cells or cells of the capsule) at the bottom of the capsule (3). Overlying the lumen is a cellular cap, attached with tight junctions to the walls of the capsule, which may serve to control the ionic environment of the lumen (4). Loose cellular tissue fills the capsule above the cap. A continuous layer of epidermal cells covers the electroreceptors.

Synaptic contact exists between the electroreceptor cells' inner membranes and an afferent fiber. In Gymnotid fish, anatomical (5) and electrophysiological (1) evidence suggests that the synapses are chemical. (The tuberous electroreceptor synapse of the highest frequency

Dr. Olson's current address is Department of Biomedical Engineering Boston University 02215.

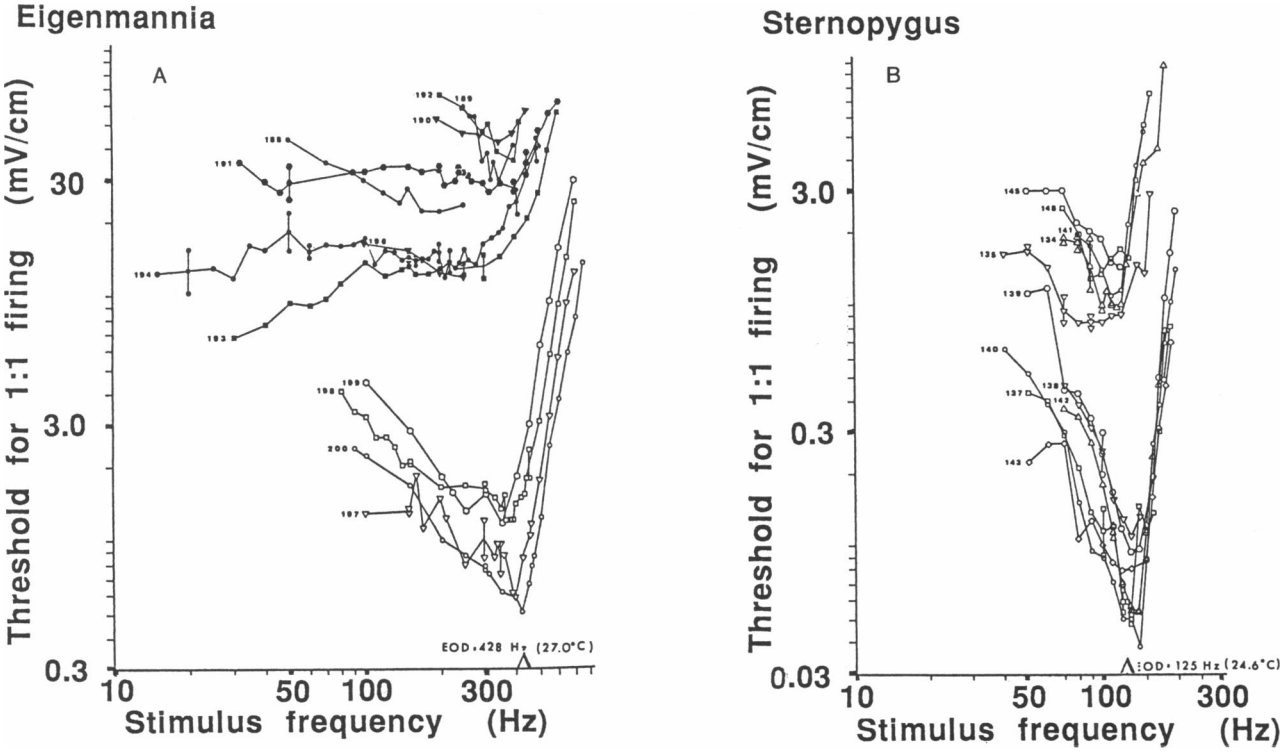

FIGURE 1 From Hopkins (2). Tuning curves for tuberous electroreceptor afferent fibers from a single Eigenmannia (*A*) and a single Sternopygus (*B*). Each curve represents a single fiber. Thresholds were determined by measuring the minimum electric field required to elicit one spike on each stimulus cycle (1:1 firing). Arrows identify EOD frequencies of the fish, measured before the experiments.

Gymnotid fish, Apteronotus, might employ both electrical and chemical transmission [6].) One afferent fiber contacts all the receptor cells within an organ, and when the receptors exist in a cluster, one afferent contacts all the receptor cells within the cluster.

From the anatomical structure of the receptors and electrophysiological measurements, Bennett proposed that the electrical behavior could be described by the equivalent circuit in Fig. 2 *a*, (1). Based on his measurements of damped and sustained electroreceptor oscillations he proposed that the inner, innervated membrane of the electroreceptor cells contained active conductances that resonate at a particular frequency. (Zakon [1986] supported this proposal by showing that channel blocking agents can block oscillations when applied to the inner membranes [7].) The fact that the system is insensitive to dc stimulus was explained by representing the outer membrane by a capacitor that provided the dc block.

We performed measurements of the impedance of the tuberous-electroreceptor/skin structure of the electric fish Eigenmannia, with EOD frequencies (varying from fish to fish) between 200 and 400 Hz, and Sternopygus, with EOD frequencies between 50 and 200 Hz. The current levels used were chosen to produce transdermal

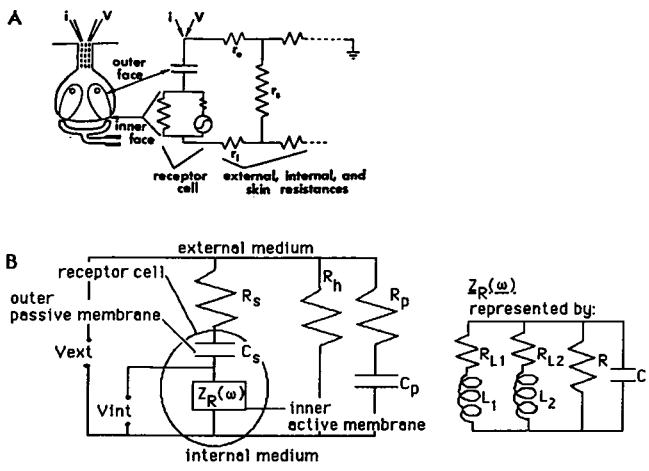

FIGURE 2 (*A*) From Bennett (1). Anatomical diagram and equivalent circuit of tuberous electroreceptor. Bennett's stimulation and recording electrodes are indicated. (*B*) Our quantitative circuit model of the structure. R_h, R_p, and C_p represent skin adjacent to the receptors. R_s represents the resistance of tissue and a cellular cap that overlie the receptor cells. The receptor cells' outer (passive) membranes are modeled as a capacitor, C_s, the inner (active) membranes as a parallel resonant circuit with frequency dependent impedance $Z_R(\omega)$.

voltages similar in magnitude to the transdermal voltage produced by the EOD, on the order of 1 mV. A frequency dependent impedance tuned close to the EOD frequency of the individual fish is in evidence in our data. We used our resonance measurements, measurements over receptorless skin, and anatomically and physiologically based estimates to construct an equivalent circuit model of the tuberous-electroreceptor/skin structure, and used the model to estimate the frequency selectivity that is provided by the electroreceptor. The model is a linear approximation of the electroreceptor/skin structure. The 1 mV transdermal voltage produced in our measurements is small compared with the operating voltages of known active membranes, justifying the attempt at a linear description. The linear model served to describe many of our measurements, in which voltage scaled linearly with current. In some cases however, the system displayed active nonlinearity, first noticed in the form of sustained voltage oscillations. With sinusoidal current drive, nonlinear units showed current-level dependence in the shape (sharpness) of their tuned impedance. Qualitative features of the observed active nonlinearity can be reproduced using a generalized description of active membrane conductances: from a description representing conductances operating in a stable, linear regime, to a description representing conductances poised between stability and instability.

The experiments and analysis described are not a substitute for direct investigations on the electroreceptor cell membrane conductances that produce the impedance resonance. Such investigations would best be performed with intracellular and patch clamp recordings of individual electroreceptor cells. The transdermal measurements we performed are relevant to understanding the frequency selectivity that is provided by the electroreceptor resonance. The electroreceptor operates within a structure, the surrounding tissue, which, by providing current paths in series and parallel with the electroreceptors, influences the frequency selectivity that is produced by the resonant impedance of the electroreceptor membrane. Understanding the frequency selectivity of the electroreceptor system cannot be accomplished solely with intracellular and patch clamp studies, which would disturb the surrounding tissue.

Interpretation of our data was based upon Bennett's qualitative model. The success with which the model could be developed into a quantitative form capable of reproducing experimental results strengthened the credibility of the model.

B. METHODS

Measurements were performed with the fish's EOD silenced by an injection of gallamine triethiodide (Flaxedil; American Cyanamid Co., Danbury, CT), which blocks the activity of muscle tissue and the electric organ without affecting nerve or receptor behavior. Flaxedil, which is sold in a 20 mg/ml dilution, was diluted with Hartmann's Ringer solution. Dosages varied with the size of the fish. The average dose for a 9 cm Eigenmannia was 8 μg; the average dose for a 16 cm Sternopygus was 100 μg. Sometimes additional injections were necessary during an experiment. Except for the injection, experiments were noninvasive. Sternopygus usually recovered fully a few hours after an experiment and could be used in multiple experiments. Eigenmannia are delicate and because of unavoidable handling they often did not recover fully, and died hours to days after an experiment.

During an experiment the fish was completely submerged in a shallow plastic tub filled with tank water. The tank water had a resistivity of 1–2 kΩ-cm and a pH of ~6.8. Bath temperature was maintained at 26°C. The water was electrically grounded. The fish was respirated by means of a tube placed in its mouth through which aerated water flowed continuously. A ground wire was coiled around the end of the tube in the fish's mouth.

The impedance of the receptor/skin structure was measured in regions of high receptor density: on the head, or over a cluster of receptors in the trunk. A known current stimulus was delivered and voltage measured. A signal generator in series with a large (10 or 18 MΩ) resistor approximated a current source. The current source was attached to a silver wire in a glass capillary that was filled with tank water. Current was passed through the tip of the capillary, which was pressed against the skin of the fish, through the skin to the inner milieu of the fish, at ground. The voltage was measured at the tip of the capillary with a silver probe wire, insulated to its tip.

Current was limited to a controlled area of skin by one of two sealing methods: either an electrical guard seal, or a mechanical seal. The mechanical seal, which isolated an area of ~0.5 mm^2 (covering roughly 30 tuberous electroreceptors in a high density region) used an unpulled fire polished capillary, with a thin layer of silicone sealer applied to its tip. When the tip was pressed gently against the skin, current was prevented from shunting between the capillary and the bath, and passed through the patch of skin subtended by the tip of the capillary. The design of the guard ring probe is shown in Fig. 3. The electrical guard sealing method, isolating a 0.05 mm^2 area, (covering roughly three to five electroreceptors in a high density region or in a cluster) prevented

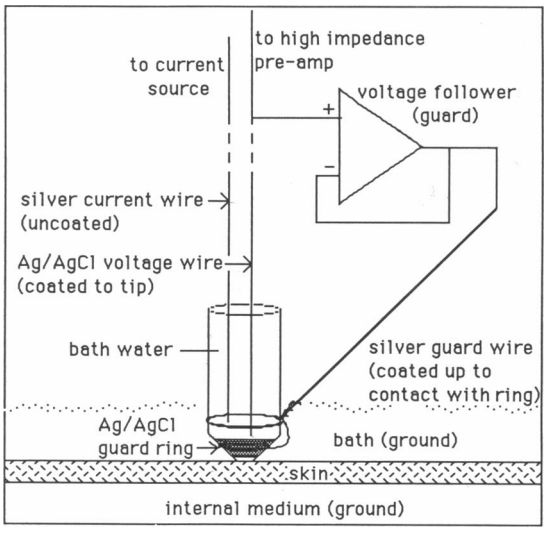

FIGURE 3 Guard ring probe.

current leakage by means of electrical feedback. The voltage measured at the tip of the guard ring capillary by the voltage probe was fed into a voltage follower. A voltage follower is a single operational amplifier with negative feedback, which supplies the current necessary to maintain its output voltage equal to its input voltage. The output of the follower was applied to a guard ring just outside the hole of the capillary. Because the voltages to be reproduced were small, an Op-07 op-amp, which has low voltage and current offsets (dc errors), was used. The guard ring maintained the voltage immediately outside the capillary at the voltage measured at the tip inside the capillary. Therefore no current leaked to the bath and the current was focussed through the skin. Unless noted, the data presented are from measurements performed with the electrical guard probe.

Current stimulus levels were set so that the maximum voltage across the skin was ~1 mV, approximately the natural stimulus level due to the EOD. For the small probe, this corresponded to current amplitudes in the range between a fraction of a nanoamp and single nanoamps. With a swept frequency, constant amplitude current drive the magnitude of the transdermal voltage, $|V_{ext}(\omega)|$, was measured. (A typical sweep speed was 40 Hz/s.) Thus, we computed $|Z_{ext}(\omega)| = |V_{ext}(\omega)|/I$ for the linear model. We also measured V_{ext} (magnitude and phase relative to I) at several fixed frequencies to give the complex value of $Z_{ext}(\omega)$ at these frequencies. Finally, the impulse response evoked by a 1–2 ms current pulse was recorded at many probe locations.

C. RESULTS AND ANALYSIS

1. Linear observations and description

Experimental observations

A typical swept-frequency voltage measurement from Eigenmannia is shown in Fig. 4, along with this unit's impulse response. The fish's f_{EOD} was in this case 250 Hz. The ringing impulse response speaks for resonant conductances in the electroreceptor cell membrane. Qualitative features of the swept-frequency impedance measurement reflect interactions between specific admittances. The voltage peak at 225 Hz indicates the presence of a parallel resonance at this frequency. In general, the voltage peaks were within 15% of the EOD frequency, measured at the beginning of experiments. The voltage valley at 175 Hz suggests a series resonance, plausibly between an inductive admittance (such as can be produced by an active membrane conductance) in the electroreceptor cells' inner membranes, and the capacitance of the outer membranes. At frequencies below 175 Hz the monotonic voltage increase reflects capacitance, and speaks for the dc block that has been attributed to the receptor cells' outer membrane capacitance. In Fig. 5, the current-stimulus sinusoid and voltage response of another unit (in a different fish) are displayed at frequencies above, below, and close to the peak-voltage frequency. The voltage waveform has the appearance of a pure sinusoid. These discrete frequency data show the phase between the stimulus (current) and response (voltage) sinusoids.

Experiments performed on Sternopygus supported the linear description of the active membrane conductances. Linearity is demonstrated by linear scaling of voltage with current, both in the swept-frequency impedance and in the ringing impulse response. Fig. 6 shows swept-frequency voltage responses at two current levels from a unit in a Sternopygus with f_{EOD} = 140 Hz. The frequency dependent impedance magnitudes of the two responses are close to equal. Data from experiments on Eigenmannia sometimes displayed active nonlinearity in the form of

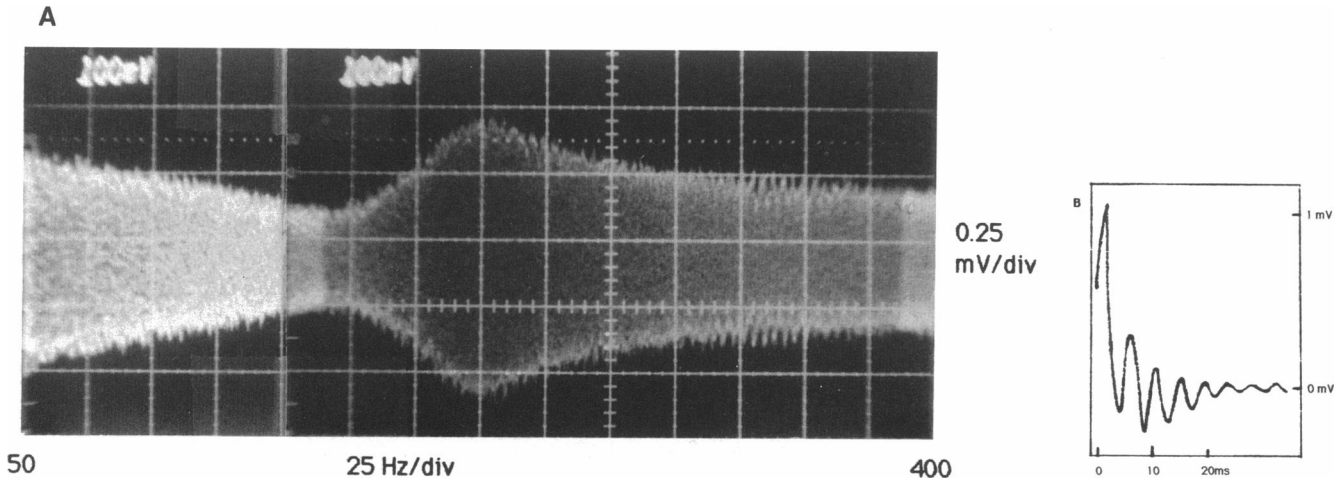

FIGURE 4 (*A*) Swept-frequency voltage response. Stimulus was 0.6 namp peak-to-peak sinusoidal current with frequency that swept from 50 to 400 Hz. (*B*) Voltage response (same unit as in *A*) to 1 namp, 2 ms current pulse. Frequency of damped oscillation is ~215 Hz. Fish's f_{EOD} = 250 Hz. Data taken with small probe.

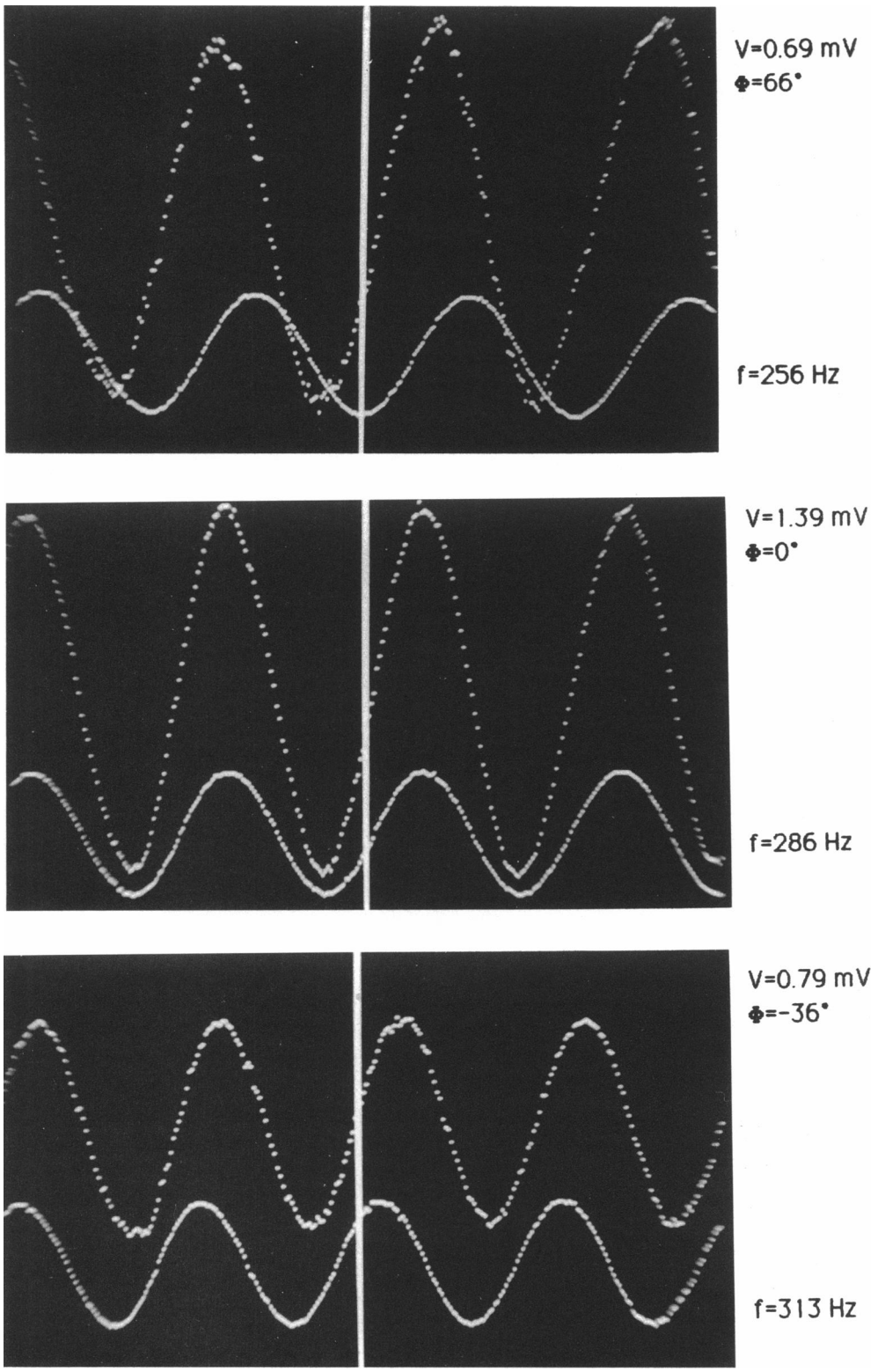

FIGURE 5 Voltage response to 0.28 namp sinusoidal current. As stimulus frequency is stepped through the peak-voltage frequency at 295 Hz, phase of voltage (*upper trace* in each photo) relative to current (*lower trace* in each photo) goes from positive to negative. (V = peak-to-peak voltage. Voltage amplification is greater in the upper photo than in the other two photos.) Fish's f_{BOD} = 300 Hz. Data taken with small probe.

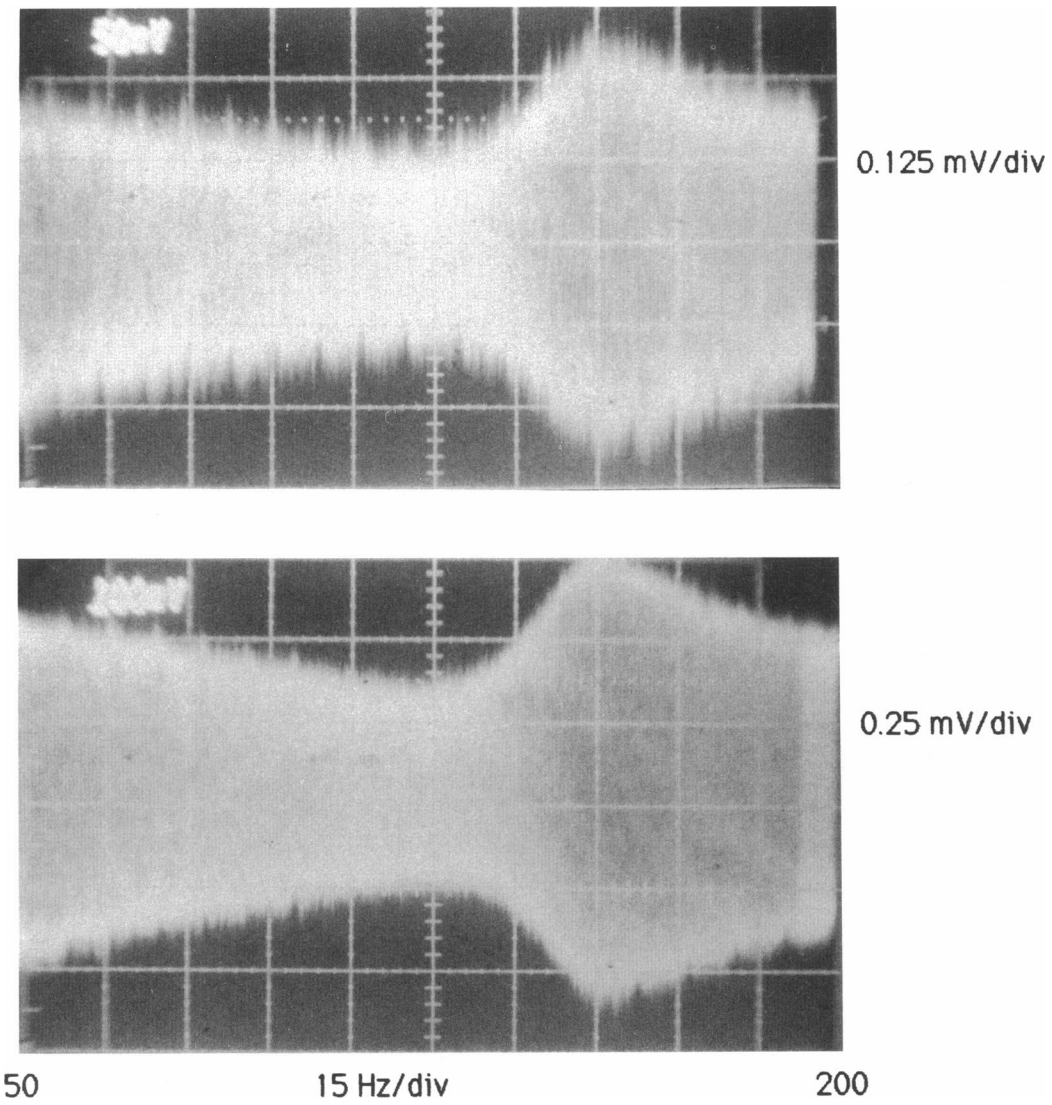

FIGURE 6 Swept-frequency voltage responses from Sternopygus at two stimulus levels. Current level is 0.25 namp peak-to-peak in the upper trace, 0.56 namp peak-to-peak in the lower trace. Fish's f_{EOD} = 140 Hz. Data taken with small probe.

sustained voltage oscillations, and level dependent resonance sharpness even at low stimulus levels.

2. The model

a. Structure surrounding the electroreceptors

The equivalent circuit model of the electroreceptor/skin structure is shown in Fig. 2 *b*. The skin is capacitive as well as resistive, and we model the skin adjacent to the receptors with the circuit elements R_h, R_p, and C_p. The approximate values of R_h, R_p, and C_p were determined from measurements over receptorless skin. The values of R_h, R_p, and C_p were adjusted to match the experimental data, with results shown in Fig. 7. The computed impedance magnitude and phase, plotted as continuous curves, are compared with the data, which are plotted as crosses. In five measurements of skin impedance, made on different days and thus with some variability in probe area (probe area = 0.05 mm^2 ± 25%) the values assumed by R_h, R_p, and C_p had the following means and ranges: R_h: range = 0.9 – 2.4 MΩ, mean = 1.6 MΩ; R_p: range = 0.7 – 2.2 MΩ, mean = 1.2 MΩ; C_p: range = 125–420 pF, mean = 277 pF. The impedance magnitude agrees fairly well with Bennett's value of the dc impedance of the skin of Gymnotid fish, which he estimated to be 1–3 kΩ-cm^2.

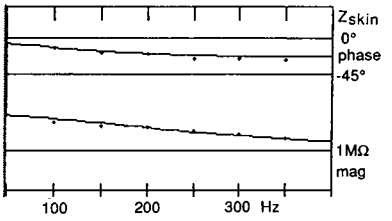

FIGURE 7 Phase and magnitude data from a skin impedance measurement are plotted as crosses. The continuous lines that go roughly through the data points are the phase and magnitude of the skin circuit with $R_h = 1.9 \times 10^6\ \Omega$, $R_p = 1.5 \times 10^6\ \Omega$, $C_p = 1.9 \times 10^{-10}\ F$.

The capacitance value can be used to calculate an order of magnitude estimate of the dielectric constant of the fish's skin. Approximating the skin as a homogenous layer of material with dielectric constant ϵ, $\epsilon = Cd/A$ where C is the capacitance, d is the thickness of the skin, and A is the probe area. By examining a fish slice under a microscope we approximated the skin thickness to be 0.05 mm. Thus $\epsilon \approx 3 \times 10^{-7}$ F/m, or $3 \times 10^4\ \epsilon_0$. This seemingly large dielectric constant (water is 80 ϵ_0) is realistic when compared with the known dielectric constants of cellular tissue. For example, muscle tissue has $\epsilon \approx 10^3\ \epsilon_0$ at frequencies in the range of hundreds to thousands of Hz. In addition, the capacitance of frog skin, reported as 1.8 μF/cm^2, is the same order of magnitude as the 0.6 μF/cm^2 capacitance of the fish skin (8). R_s, a resistor in series with the electroreceptors, represents the series resistance of a cellular cap that overlies the receptor cells, and tissue that overlies the receptor.

b. Electroreceptors

In the model, we treat all the receptor cells contained in one electroreceptor organ as one (correspondingly large) receptor cell. Anatomical justification for this treatment lies in the large size and resultant large capacitance of the receptor cell outer membrane, which would provide close to an ac short circuit between adjacent receptor cells. We extend the lumped treatment to include all the electroreceptors subtended in a single measurement. This approximation rests on an assumption of coherence in electroreceptor activity when a group of electroreceptors is isolated and given uniform stimulation. Impedance measurements made with the small and large probe differed in their subtended areas, and number of subtended electroreceptors, by a factor of 10. Features of the electroreceptor/skin impedance in large probe measurements were similar in detail to the impedance in small probe measurements, suggesting that we measure a coherent response. The outer membrane is modeled as a capacitor, C_s, with a capacitance value of ~1 μF per cm^2 of outer membrane area. The small probe subtends three to five electroreceptors, corresponding to ~80 electroreceptor cells. The outer membrane area of one electroreceptor cell is 10^{-5} cm^2, so the outer membrane area of 80 cells is $\sim 0.8 \times 10^{-3}$ cm^2. This gives a predicted outer membrane capacitance of ~0.8 nF.

The inner membrane is modeled as a resonant circuit. The active ionic conductances responsible for tuberous electroreceptor tuning are unknown. Zakon has observed that K^+ and Ca^{++} are necessary for an oscillatory impulse response (7) and Zipser and Bennett showed that Na^+ is probably not involved in the resonance mechanism (9). Our measurements do not give information about the individual conductances that give rise to the membrane resonance, but they do provide general constraints on the individual conductances. A requirement on the active membrane is that it possess conductances that resonate at the frequency of the impedance maximum. A second requirement is for a regenerative conductance, which can provide the negative resistance that sometimes produces instability in the electroreceptors.

Our stimulus was set near the transdermal voltage of the natural EOD stimulus, at ~1 mV. This is small compared with the voltage range of known active channels, encouraging a perturbation (linear) approximation of active membrane impedance. In a linear approximation the equations governing voltage dependent conductances are linearized about the membrane's equilibrium voltage. The resulting equations can be shown to be the same as for a parallel L-C-R circuit. This was first described by Hodgkin and Huxley (10) and was explored in detail by Mauro et al (11). They showed that a nonregenerative channel can be represented by a resistor in series with an inductor, these in parallel with a resistor. A regenerative channel has the same form, with the series resistor and inductor taking negative values. In both, the activation rate of the channel (evaluated at the equilibrium voltage) is equal to the ratio of the series resistor to the series inductor. In the simplest resonant membrane description, resonance is produced between a nonregenerative channel and the passive membrane capacitance. (Basically an L-C resonance.) Alternatively, resonance can be produced between a regenerative and a nonregenerative channel. We tried the linearized forms of these alternative descriptions to produce an active membrane impedance, defined as $Z_R(\omega)$, that would lead to an accurate fit of our transdermal impedance data. We found that both models were capable of producing the $Z_R(\omega)$ that would produce an accurate fit to the data. However, the simplest (L-C) model was found to call for an inner membrane capacitance of 25–35 μF per cm^2 of inner membrane area. This value is unrealistically large for passive membrane capacitance, and the L-C model was rejected as physically

implausible. The alternative active membrane model, with resonance produced by the interaction between a regenerative and nonregenerative channel, was able to produce the necessary $Z_R(\omega)$ with physically reasonable conductances, and was employed in the system model. This active membrane model, shown in Fig. 2 *b*, is composed of the following elements in parallel: a resistor in series with an inductor, representing the active component of the nonregenerative channel and denoted by R_{L1} and L_1; a resistor in series with an inductor, representing the active component of the regenerative channel and denoted by R_{L2} and L_2; R, representing leakage conductance and the passive components of the active conductances; C, representing passive membrane capacitance.

We do not forward our model as accurately describing the specific conductances in the active membrane. Our goal is to determine the tuning produced by the resonant impedance, and for this, the impedance function $Z_R(\omega)$ is what must be accurate. Because linearization loses all but the first order properties of a system, different active conductances, even conductances governed by ion concentration instead of voltage, can give rise to identical linearized forms (12). This, coupled with the observation above that different linearized forms can produce nearly identical resonant impedances ($Z_R[\omega]$) reduces our discomfort in attributing a specific form to the active membrane.

3. Model fit to the data

The model was fit to the data by fitting the magnitude of the impedance of the equivalent circuit to the swept-frequency impedance magnitude data. The values of the parameters R_h, R_p, C_p, and C_s were constrained as described above. The model's fit to the data of Fig. 4 is shown in Fig. 8 *a*; the model's fit to the data of Fig. 6 is in Fig. 8 *c*. The experimental values of the impedance magnitude (taken from a swept-frequency curve) and phase are plotted as crosses. The continuous lines that go roughly through the data points are the phase and magnitude of the impedance of the equivalent circuit model. In Fig. 8 *b*, the Fig. 4 model's response to a current pulse is similar to the pulse response the unit displayed.

Parameters of the active membrane

The inner membrane area of 80 electroreceptor cells (roughly the number subtended by the small probe) is 3×10^{-5} cm^2. The inner membrane capacitance was assumed to be equal to the outer membrane capacitance multiplied by the ratio of the inner to outer membrane area, and was found to be an unimportant admittance through the membrane at EOD frequencies. After being normalized to inner membrane area the nonregenerative and regenerative channels from the model representing the Fig. 4

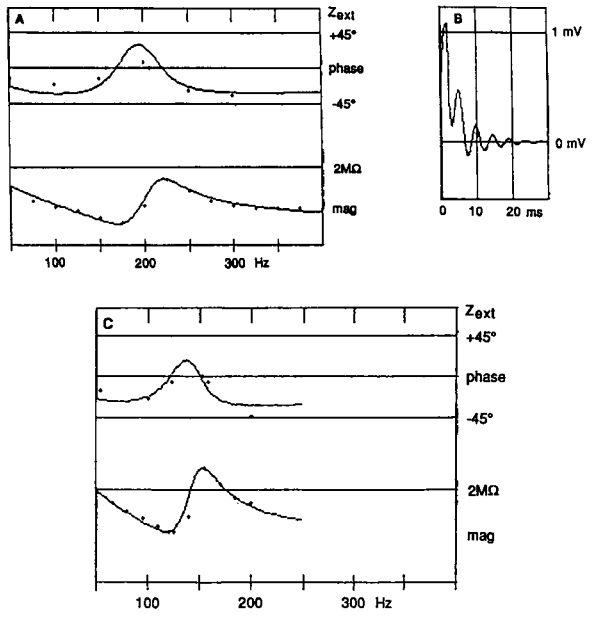

FIGURE 8 (*A*) Impedance magnitude and phase produced by equivalent circuit with parameters chosen to fit data in Fig. 4, compared with data (plotted as crosses). Parameters: R_h = 1.8 MΩ, R_p = 1.5 MΩ, C_p = 50 pF, R_s = 0.8 MΩ, C_s = 810 pF, R = 0.20 MΩ, C = 41 pF, R_{L1} = 0.077 MΩ, L_1 = 440 H, R_{L2} = −0.18 MΩ, L_2 = −35 H. (*B*) Calculated response of equivalent circuit of *A* to 1 namp, 2 ms current pulse. (*C*) Impedance magnitude and phase produced by equivalent circuit with parameters chosen to fit data in Fig. 6, compared with data (plotted as crosses). Parameters: R_h = 2.6 MΩ, R_p = 2.5 MΩ, C_p = 100 pF, R_s = 1.8 MΩ, C_s = 610 pF, R = 0.25 MΩ, C = 31 pF, R_{L1} = 0.20 MΩ, L_1 = 1,200 H, R_{L2} = −0.24 MΩ, L_2 = −47 H.

data have asymptotic resistance values (found by multiplying R_{L1} and R_{L2} by the total inner membrane area) of 2.4 Ω-cm^2 and −5.4 Ω-cm^2, respectively. These values are plausible when compared with active resistance values from the literature. For example, the active conductances in the receptor cells of the Ampulla of Lorenzini, low frequency electroreceptors of skates, have resistance values of 4.9 ± 2.4 Ω-cm^2 and −38 ± 5 Ω-cm^2 (13). In the model that represents the Fig. 4 data the activation rate of the nonregenerative channel (R_{L1}/L_1) was 175 Hz and of the regenerative channel (R_{L2}/L_2) was 5,000 Hz. These activation rates are plausible based on known channel activation rates.

4. Estimating electroreceptor selectivity

Referring to the diagram of the model in Fig. 2 *b*, V_{ext}, the voltage we measure, and V_{int}, the voltage across the active membrane, are identified. $V_{ext} = I \times Z_T$, where Z_T is the impedance of the whole structure. With $Z_R(\omega)$ equal to the impedance of the active membrane and $Z_s(\omega)$ equal to the series impedance of R_s and C_s, $V_{int} = V_{ext} \times Z_R/$

$(Z_s + Z_R)$. We define Z_{int}: $Z_{int} = V_{int}/I = Z_R Z_T/(Z_s + Z_R)$. Z_{int} is the quantity that relates the external stimulus current to the voltage across the electroreceptor innervated membrane. The series and shunt impedances of the structure surrounding the active membrane influence the voltage across the membrane, and thus influence the selectivity provided by the membrane's electrical resonance. The shunt impedance of surrounding skin damps the resonance. The series impedance, Z_s, provides some isolation of the resonant impedance from the shunt. In Fig. 9, $Z_{int}(\omega)$ is plotted for the circuit model that fits the Fig. 4 data. Comparing Fig. 9 with Fig. 8 *a*, in which the Z_{ext} data and model fit are plotted, it is seen that at resonance, $|Z_{int}| \approx |Z_{ext}|$. The active membrane impedance greatly dominates the series impedance at the most selective frequency. At frequencies below the resonant frequency, Z_R decreases while Z_s increases, serving to decrease the proportion of V_{ext} developed across Z_R. This increased isolation enhances low frequency selectivity. In contrast, on the high frequency side of resonance Z_R and Z_s both decrease. At high frequencies the active membrane is comparatively less isolated from V_{ext}, and the selectivity provided by Z_R is consequently diminished.

The frequency dependence of $|Z_{int}|$ gives the frequency selectivity of the electroreceptor. In analogy with the neural data, which are presented as a log–log plot of (field strength necessary to elicit one spike per cycle) versus frequency, the $|Z_{int}|$ prediction can be presented as a log–log plot of $|Z_{int}|^{-1}$, versus frequency. Because $I = V_{int}/Z_{int}$, this gives a tuning curve of the current necessary to attain a threshold $|V_{int}|$.

Fig. 10 illustrates the tuning curves predicted by the model for the Eigenmannia measurement of Fig. 4 and the Sternopygus measurement of Fig. 6. The dashed horizontal lines indicate the 10 dB bandwidth of each curve. The number given by the ratio of the best frequency to the 10 dB bandwidth, $f_0/\Delta f_{10dB}$, characterizes the selectivity of the tip of the tuning curves. For the

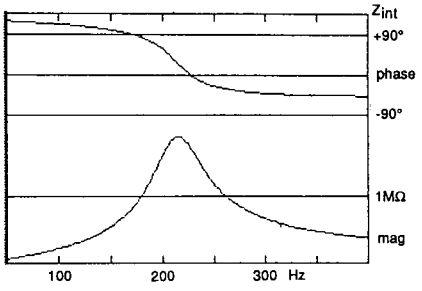

FIGURE 9 Magnitude and phase of $Z_{int}(\omega)$, the quantity that relates electroreceptor voltage to stimulus current, produced by the equivalent circuit of Fig. 8 *a*.

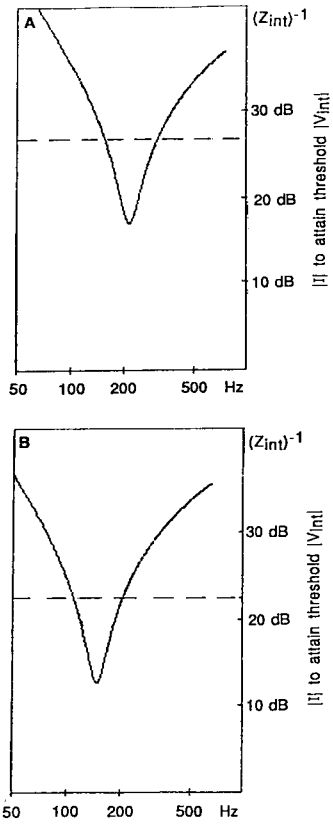

FIGURE 10 Estimation of electroreceptor selectivity. Tuning curves produced by the equivalent circuits corresponding to data of Fig. 4 *A* and Fig. 6 *B*. Dashed lines are 10 dB from curve tips.

data of Fig. 4, $f_0/\Delta f_{10dB} = 1.5$; for the data of Fig. 6, $f_0/\Delta f_{10dB} = 1.55$. These $f_0/\Delta f_{10dB}$ values are typical of our measurements of linear electroreceptor impedance. In comparison, the sharpest neural selectivity curves in Fig. 1 have $f_0/\Delta f_{10dB}$ values of 1.9 (Sternopygus) and 1.25 (Eigenmannia). According to the $f_0/\Delta f_{10dB}$ values, the neural selectivity and our estimations of electroreceptor selectivity are in reasonable agreement. In units that displayed active nonlinearity, the impedance sharpness could be much greater, with $f_0/\Delta f_{10dB}$ values up to 4.5.

At frequencies above the most sensitive frequency, the Z_{int} tuning curves level off, and the agreement with the neural tuning curves diminishes. The asymptotic behavior of $Z_{int}(\omega)$ is inherent in the resonant circuit model. At the resonant frequency, the impedance can be very large, and the fall-off in impedance for frequencies close to the resonant frequency can be sharp. But at frequencies far from the resonant frequency, the impedance is governed by individual conductances, which produce high and low frequency fall-offs of 20 dB/decade or less. To bring the predicted tuning and the neural tuning curves into better agreement, several low-pass filters are required in con-

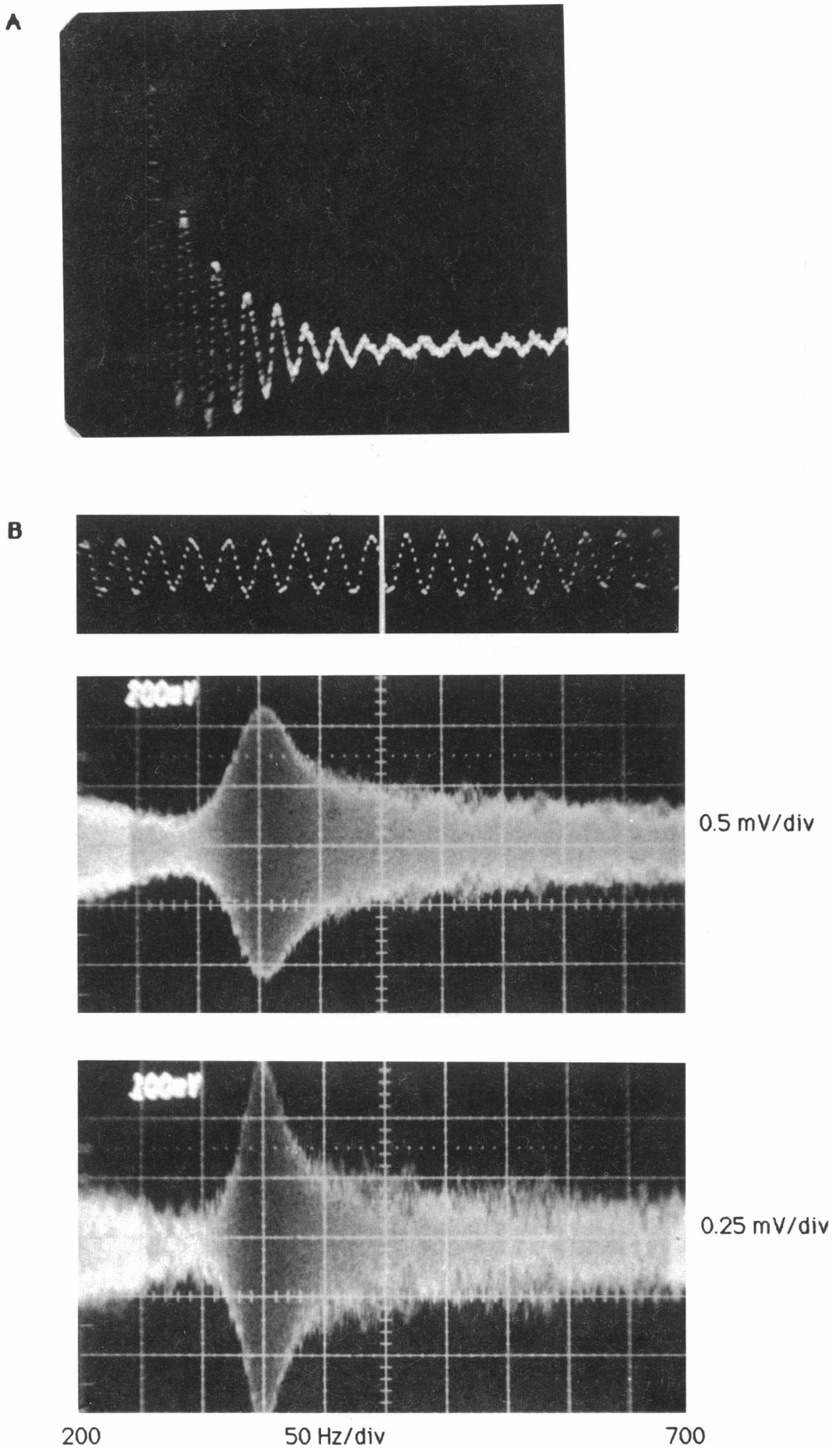

FIGURE 11 (*continued*)

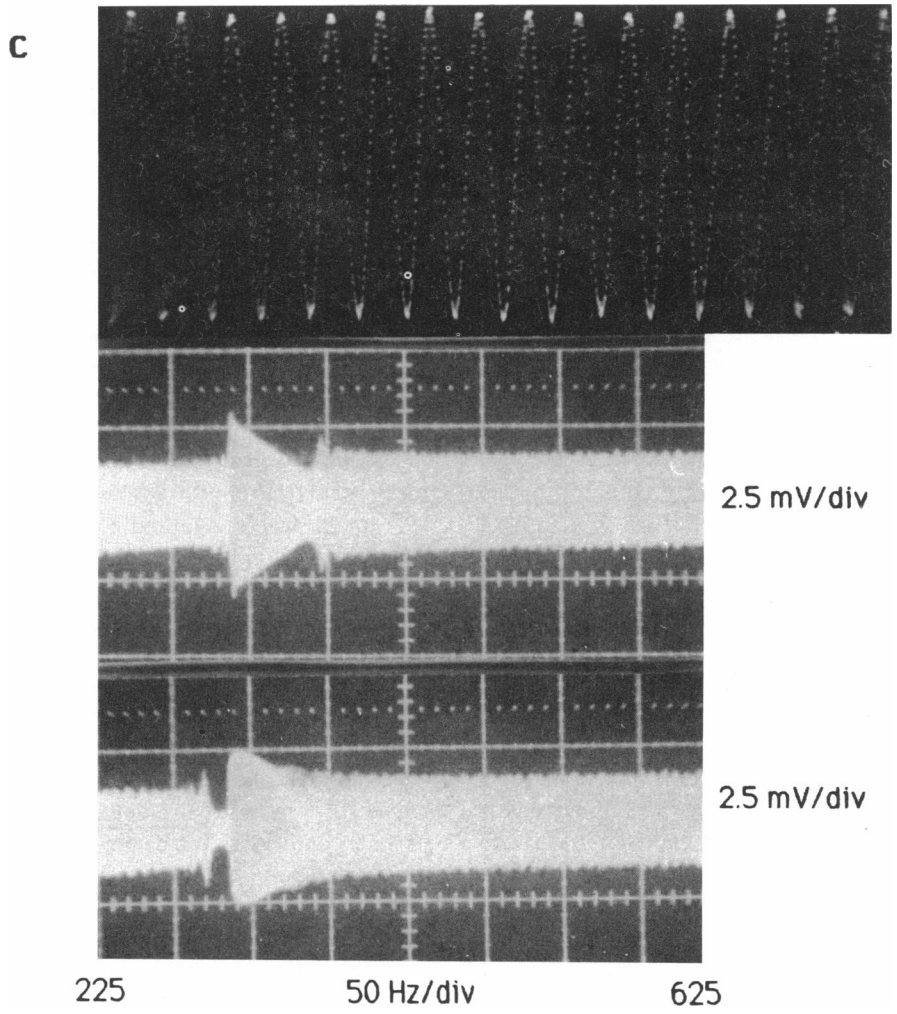

FIGURE 11 (*A*) 2 ms, 0.83 namp current pulse caused 1.15 mV response that decayed to a 0.07 mV sustained oscillation. Sustained oscillation frequency = 278 Hz, damped oscillation frequency = 270 Hz. Fish's EOD frequency was 290 Hz. (Data taken with small probe). (*B*) Unit with 351 Hz, 0.58 mV spontaneous oscillation in top trace displayed nonlinear scaling of voltage with current. Middle trace shows swept-frequency voltage response to sinusoidal 0.56 namp drive, swept between 200 and 700 Hz. Lower trace shows response when drive amplitude is reduced by a factor of two. Because oscilloscope gain is increased by a factor of two in the lower trace, if voltage scaled linearly with current, the two traces would be identical. Fish's EOD frequency was 400 Hz. (Data taken with small probe.) (*C*) Unit with 2.5 mV, 327 Hz spontaneous oscillation in top trace displayed limit cycle quenching when driven at frequencies close to the limit cycle frequency. At sweep speed used response showed hysteresis, so sweeps both increasing and decreasing in frequency are shown. Drive amplitude was 0.56 namp. For increasing frequency (*middle trace*), response entrained to the drive just at maximum voltage frequency (317 Hz), remained entrained to 365 Hz where limit cycle reasserted itself. For decreasing frequency (*lower trace*), response entrained at 340 Hz, grew to maximum voltage at 317 Hz, and then collapsed, but remained entrained to drive to 300 Hz, where limit cycle took over. (Data taken will small probe.)

catenation with the resonant filtering we have discussed. Such low-pass filtering might be found in the chemical synapse. Investigations of the filtering properties of chemical synapses are in Llinas et al. (14,15) and Kidd (16), where equivalent low-pass filters are proposed.

D. Active nonlinearity in electroreceptor behavior

The linear approximation of active membrane equations employed above served to model the active electroreceptor cell membrane in many of our measurements, in which voltage scaled linearly with current, and pulse induced voltage ringing damped to zero. In some cases, however, our measurements displayed active nonlinearity in the form of sustained voltage oscillations, and voltage-dependent resonant impedance sharpness at low stimulus levels. The nonlinear behavior we observed could be explained in terms of a system in limit cycle (17). To be capable of limit cycle behavior a resonant membrane must possess a component of negative conductance, (such as can be

provided by an active, regenerative conductance). A negative conductance provides a resonant membrane with a component of negative damping. If the negative damping of the negative conductance is dominated by the positive damping of positive conductances at equilibrium, the system will be stable, will not oscillate spontaneously, and may be approximated as a linear system for perturbations (possibly very small) from equilibrium. If negative damping exceeds positive damping at equilibrium, the system will be unstable, and might undergo a sustained oscillation about its equilibrium point. In nonlinear dynamics such an oscillation is called a limit cycle. In a linear treatment, damping is approximated as being independent of voltage. For a system in limit cycle, the approximation is invalid; damping is negative at voltages smaller than, and positive at voltages greater than, the limit cycle voltage. The near-cancellation of damping terms produces strongly voltage dependent damping close to the equilibrium voltage. In our measurements, level dependent damping was observed in the stimulus-level dependent impedance of oscillating, as well as of some nonoscillating electroreceptors.

A quantitative study of an active membrane that displayed limit cycle oscillations was done by Morris and Lecar (18). They did not examine the response of their system to sinusoidal current drive, and we undertook a numerical analysis of their equations and found that the response to sinusoidal current drive paralleled our observations of the nonlinear electroreceptor response to sinusoidal drive. This behavior includes harmonic entrainment, limit cycle entrainment, and nonlinear scaling at very low stimulus levels. These phenomenon, which are common to many nonlinear oscillatory systems, are described more generally in Hayashi's book (17). Below, we describe our observations of active nonlinearity in electroreceptors.

1. Experimental observations

Active nonlinearity was only significant in measurements on Eigenmannia, where over 50% of the electroreceptor recordings displayed spontaneous oscillations. Small (0.05 mV maximum) oscillations were rarely detected with Sternopygus, and even when oscillations were present, the resonant impedance did not display level-dependent sharpness down to the minimum transdermal voltage levels set by the noise limitations of our experiments (0.02 mV).

a. Oscillations

In Fig. 11 *a* the voltage oscillation after a current pulse damps not to zero, but to a 0.07 mV sustained oscillation. We have established in two ways that the sustained oscillations we measured were generated at the same site as the damped oscillations that occurred in response to a current pulse. First, a small displacement of the probe caused both the damped and the sustained oscillations to disappear, indicating that they had been generated at the same position. Second, the frequency of a sustained oscillation was equal to, or slightly greater than, the frequency of the damped oscillation: the two frequencies were definitely correlated. A sampling of ten units from several different fish, with damped oscillation frequencies that ranged between 243 and 417 Hz, displayed spontaneous oscillations with frequencies that were greater than their damped oscillation frequencies by an average of 4%. The maximum frequency difference was 11%, and the minimum was zero.

With the large probe (subtending ~50 electroreceptors) oscillation amplitudes were up to 0.07 mV. When the small probe (subtending ~5 electroreceptors) was used, the variability in amplitude was much greater, with a maximum voltage of 2.5 mV. In several cases the oscillation amplitude suddenly increased while being recorded. Usually oscillations appeared as though they had been generated by a single source (with either probe), although in a few cases beats were seen.

We explored the possibility that the electroreceptors became unstable only during the isolation that is introduced by the measurements, and were stable under natural conditions. We performed the following measurements on several spontaneously oscillating units. With the electrical guard probe, a relatively small resistor was connected between the voltage probe wire and ground, which shunts the electroreceptor/skin structure, and thus reduces the isolation. The shunt caused a reduction in the amplitude of the oscillations, but even when the resistor was one fourth the magnitude of the impedance of the unit, oscillations often persisted. (With further increases in the shunt the oscillations became indiscernible from background noise.) With the large probe, we reduced isolation by slightly raising the probe from the skin. When the probe was no longer in contact with the skin, and the resistance had been reduced from a clamped value of 0.07 MΩ, to 0.01 MΩ, oscillations were still present. From these observations it seems probable that some receptors operate in a slightly unstable regime even in the natural state. This is reinforced by the observation that spontaneous action potentials have been detected in electroreceptor afferent fibers (with the EOD silenced), occurring at a frequency close to the EOD frequency. (H. H. Zakon personal communication.)

b. Driven response: nonlinear scaling, entrainment of oscillations

Individual swept frequency impedance measurements made over units with sustained oscillations (active units) were usually qualitatively similar to impedance measure-

ments of linear, passive units, but sequences of swept frequency impedance measurements at different current levels reflected active nonlinearity via nonlinear scaling of voltage with current. This is illustrated in Fig. 11 *b*, which displays swept frequency measurements of an unstable unit at two different current drive amplitudes. With physiological current amplitudes at frequencies close to the resonant frequency, the sustained oscillations entrained to the drive frequency. Decreasing the current amplitude by half decreased the voltage in the vicinity of the peak by less than half, resulting in a sharper resonance. The sharpening of the resonant impedance at the lower stimulus level suggests that at frequencies close to the resonant frequency, damping decreased when the stimulus level decreased.

The 2.5 mV amplitude of the sustained oscillation in Fig. 11 *c* is much larger than the norm. The swept frequency impedance of this measurement has an unusually strong frequency dependent structure, and exhibits an extreme form of entrainment, referred to as quenching, in which the entrained voltage amplitude is smaller than the amplitude of the limit cycle.

Another manifestation of active nonlinearity is harmonic entrainment, whereby a drive at $2f_0$, $3f_0$ etc. (where f_0 is close to the oscillation frequency of the driven [unstable] system) elicits a large response at f_0. With a spectrum analyzer, we detected harmonic entrainment in electroreceptors (Fig. 12). Harmonic entrainment might explain an aspect of the spiking behavior in electroreceptor afferents that was observed by Hopkins (2). When stimulating at the EOD frequency, the spiking rate in many of the afferent fibers that contact electroreceptors is one spike per stimulus cycle even at very low stimulus levels. When the frequency is changed at a fixed stimulus level, 1:1 firing is no longer attained. Hopkins observed an enhancement in spike frequency at f_0, when the drive frequency was at $2f_0$ or $3f_0$. This can be explained if the membrane voltage responds at f_0 when driven at its higher harmonics.

2. Consequences of active nonlinearity for frequency tuning

In resonant membranes, damping is produced by the passive components of membrane conductances, and also via the finite activation rates of active conductances. In the electroreceptive system, damping is also produced by the impedance shunt of surrounding tissue. If uncompensated, damping imposes a limitation on resonance sharpness. The presence of a limit cycle in our measurements is evidence for a compensatory negative damping that can sharpen the resonance, and in the extreme case lead to instability of the equilibrium voltage. Our measurements showed that when driven, a spontaneously oscillating unit

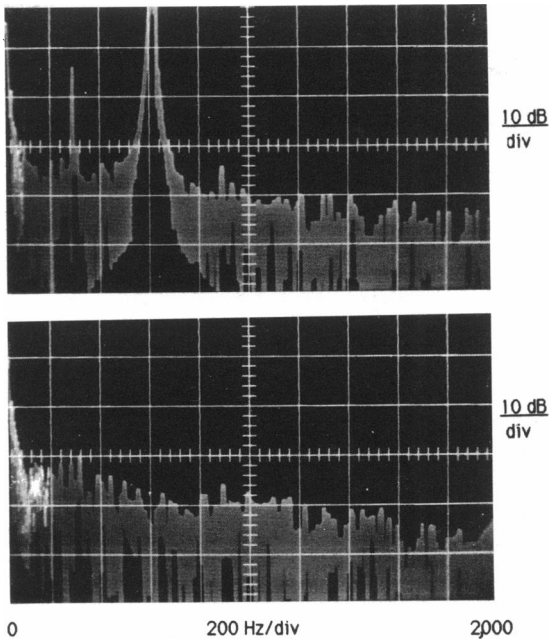

FIGURE 12 Harmonic entrainment. When unstable electroreceptor with 290 Hz resonant frequency was driven with 600 Hz, 1.1 namp sinusoidal current, frequency spectrum of external voltage had secondary spectral peak at 300 Hz. (*top photo*) Both peaks disappeared when stimulus was stopped, indicating that secondary peak was due to harmonic entrainment of electroreceptor, not just limit cycle oscillation. (Data taken with small probe.)

can become entrained to the drive, indicating that instability in the electroreceptors need not interfere with the ability to respond to the EOD.

E. SUMMARY

Transdermal measurements of electrical resonance in tuberous electroreceptors could, in many cases, be accurately reproduced with a linear equivalent circuit model of the electroreceptor/skin structure. The model allowed for a prediction of the frequency tuning that is provided by the electroreceptor when the electroreceptor is in its natural state, i.e., influenced by the series and shunt impedance of surrounding tissue. At frequencies close to the most selective frequency, the selectivity predicted by our experiments and analysis is as sharp as the selectivity known to exist neurally. The high-frequency disparity between our predicted selectivity and the neural selectivity can be reconciled if we assume several stages of low-pass filtering, which might reside in the chemical synapse between the electroreceptor cells and the afferent nerve.

In some cases the electroreceptors displayed active nonlinear behavior. The different manifestations of active

nonlinearity that appeared in our data could all be described within the framework of Hodgkin-Huxley type membrane equations, operating in a regime where membrane dissipation was poised near zero. We observed that when driven within some range of frequency spanning the oscillation frequency, most spontaneously oscillating electroreceptors became entrained to the frequency of the drive. In electric fish, the resonant frequencies of the receptors are close to the fish's f_{EOD} so the stimulus of the EOD probably entrains unstable receptors.

The authors gratefully acknowledge the contributions of J.Y. Lettuin, C.L. Searle, and H.H. Zakon to the research presented here.

This work was funded by the Whitaker Health Sciences Fund and Massachusetts Institute of Technology's Department of Computer Science and Electrical Engineering.

Received for publication 3 November 1988.

REFERENCES

1. Bennett, M. V. L. 1967. Mechanisms of electroreception. *In* Lateral Line Detectors. P. Cahn, editor. Indiana University Press, IN. 313–393.
2. Hopkins, C. 1976. Stimulus filtering and electroreception: tuberous electroreceptors in three species of gymnotoid fish. *J. Comp. Physiol.* 111:171–207.
3. Wachtel, A. W., and R. B. Szamier. 1966. Special cutaneous receptors of fish: the tuberous organs of eigenmannia. *J. Morph.* 119:51–80.
4. Zakon, H. H. 1986. The electroreceptive periphery. *In* Electroreception. T. H. Bullock and W. H. Heiligenberg, editors. John Wiley and Sons, New York.
5. Szabo, T. 1974. Anatomy of specialized lateral line organs of electroreception. *In* Handbook of Sensory Physiology III/3. A. Fessard, editor. Springer-Verlag New York, Inc., NY.
6. Srivastava, C. B. L. 1972. Morphological evidence for electrical synapse of "gap" junction type in another vertebrate receptor. *Experienta.* 28(9):1029–1030.
7. Zakon, H. 1984. The ionic basis of the oscillatory receptor potential of tuberous electroreceptors. *Soc. Neurosci.* 10:193a. (Abstr.)
8. Schanne, O. F., P. Ruiz, and E. Ceretti. 1978. Impedance measurements in epithelia: frog and toad skin. *In* Impedance Measurements in Biological Cells. John Wiley and Sons, New York.
9. Zipser, B., and M. V. L. Bennett. 1973. Tetrodotoxin resistant electrically excitable responses of receptor cells. *Brain Res.* 62:253–259.
10. Hodgkin, A. L., and A. F. Huxley. 1952. A quantitative description of membrane current and its application to conduction and excitation in nerve. *J. Physiol.* 117:500–544.
11. Mauro, A., F. Conti, F. Dodge, and R. Schor. 1970. Subthreshold behavior and phenomenological impedance of the squid giant axon. *J. Gen. Physiol.* 55:497–523.
12. Ashmore, J. F., and D. Atwell. 1985. Models for electrical tuning in hair cells. *Proc. R. Soc. Lond. B. Biol.* 26:325–354.
13. Bennett, M. V. L., and W. T. Clusin. 1978. Physiology of the ampulla of lorenzini, the Electroreceptors of elasmobranchs. *In* Sensory Biology of Sharks, Skates, and Rays. E. S. Hodgson and R. F. Mathewson, editors. Office of Naval Research.
14. Llinas, R., I. Z. Steinberg, and K. Walton. 1981*a*. Presynaptic calcium currents in squid giant synapse. *Biophys. J.* 33:289–322.
15. Llinas, R., I. Z. Steinberg, and K. Walton. 1981*b*. Relationship between presynaptic calcium current and postsynaptic potential in squid giant synapse. *Biophys. J.* 33:323–352.
16. Kidd, R. C. 1986. A Theoretical Study of the Signal Processing Properties of Ca^{++} Channel Kinetics in the Peripheral Auditory System. Masters Thesis. Massachusetts Institute of Technology, Cambridge, MA.
17. Hayashi, C. 1964. Nonlinear Oscillations in Physical Systems. McGraw Hill Inc., New York.
18. Morris, C., and H. Lecar. 1981. Voltage oscillations in the barnacle giant muscle fiber. *Biophys. J.* 35:193–213.